8 VECHINSKI, D.A., and RAO, S.M.: 'A stable procedure to calculate the transient scattering by conducting surface of arbitrary shape', *IEEE Trans.*, 1992, **AP-40**, pp. 661–665
9 RAO, S.M., and WILTON, D.R.: 'Transient scattering by conducting surfaces of arbitrary shape', *IEEE Trans.*, 1991, **AP-39**, pp. 56–61
10 ERGIN, A.A., SHANKER, B., and MICHIELSSEN, E.: 'Fast transient analysis of acoustic wave scattering from rigid bodies using a two-level plane wave time domain algorithm'. University of Illinois Research Report, November 1998

Infrared thermograms applied to near-field testing

J.M. González, A. Aguasca and J. Romeu

Electromagnetic fields close to radiant structures can be measured quickly using an infrared camera. Examples of induced fields by wire antennas over a detection screen at distances shorter than one wavelength are presented. The measured thermograms agree with simulations that take into account heat propagation on the detection screen.

Introduction: Thermograms of electromagnetic fields have demonstrated their usefulness in the measurement of fields radiated by microwave antennas [1]. The thermogram is a measurement of the infrared radiation of a detection screen with electric losses. Owing to the incident electromagnetic field a certain temperature increase is caused in the detection screen. From the infrared radiation it is possible to evaluate the electric field intensity incident on the screen. The overall measurement setup is shown in Fig. 1. Although only the field magnitude is measured, the method has potential applications in antenna testing in production processes. The main advantages are the simplicity of the measurement setup and the measurement speed. One of the main causes of errors in the measurement is the lateral conduction and convective propagation of heat along the detection screen. In this Letter we show how measurements can be improved by means of a bidimensional deconvolution with the thermal hot-spot response of the detection material. To assess the validity of the proposed deconvolution scheme the thermal images of real antennas are compared to simulated thermal images obtained by mathematical modelling which include the same heat propagation phenomena as those mentioned above.

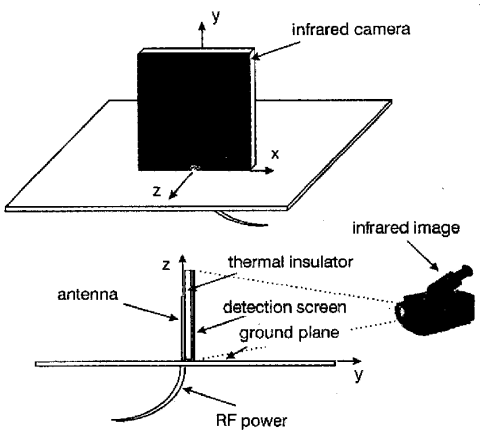

Fig. 1 *Simplified measurement setup*

Computer and RF power source not included
This Figure is shown in colour in Electronics Letters online

Theory: Infrared thermography is a technique based on the measurement of the transformation into heat of energy absorbed by a lossy material when an electromagnetic wave impinges on it. The relation between the electromagnetic fields $\vec{E}$ and $\vec{H}$ inside the material and the absorbed power for a time harmonic incident electromagnetic wave can be written as

$$P = \int_V \left(\sigma|\vec{E}|^2 + \omega\varepsilon''|\vec{E}|^2 + \omega\mu''|\vec{H}|^2\right) dV \qquad (1)$$

where σ is the conductivity of the detection screen, ε'' and μ'' are the imaginary components of the permittivity and permeability of the detection screen, and 0) is the radian frequency of the incident field. If sufficient power is absorbed by the lossy material the increase in its temperature over the environmental temperature can be detected using an infrared camera. So, from eqn. 1, materials sensitive to electric or magnetic fields could be selected or developed in accordance with the values of ε, μ and σ. The use of thin (in relation to the depth of penetration of the fields) resistive papers as detecting materials will be of great interest since they will reduce the intensity of the fields to be detected. The plane detection screen is built by attaching the resistive sheet to a thermal insulating board. In this way mechanical stiffness is provided and the efficiency of the screen is increased. Owing to the conduction, convection and radiation of heat that take place on the detection screen, the determination of its spatial thermal response to a space impulse source is needed. Analytically it could be obtained by solving the heat equation, a second-order differential equation both in space and time, with nonlinear contour conditions because of convection and radiation transfer of heat on the surface of the paper [2]. A first approach to the solution is obtained by considering small temperature increases above ambient temperature that allows a linearisation process, in the form of a modal sum. Fortunately, the impulse response could be easily represented by a bidimensional Gaussian expression with sufficient accuracy:

$$h(\vec{r}) = K \exp\left(-\frac{x^2}{2\sigma_x^2}\right)\exp\left(-\frac{y^2}{2\sigma_y^2}\right) \qquad (2)$$

The values σ_x and σ_z represent the impulse response width on the detection screen in two orthogonal axes. Both values are equal if the detection screen is horizontally located. The constant K relates the temperature increase to the power density absorbed by the screen and depends on the material and its size. To optimise the detection process by using the infrared camera a high infrared emissivity paper is of interest.

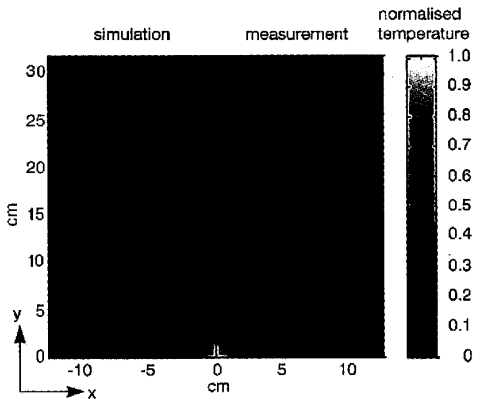

Fig. 2 *Prediction and measurement of 1.5λ monopole*

Left: prediction
Right: measurement
This Figure is shown in colour in Electronics Letters online

Detection screen and IR detector: In measurements carried out in this work we used homogeneous and isotropic carbon paper (thickness: 85 μm) as a detection screen. Owing to its electric losses, this material is an electric field detector. Its power absorption and reflection coefficients are 22 and 2%, respectively. These values were experimentally determined from measurements in a rectangular waveguide at 2.45GHz. The temperature steady-state reponse to a constant power excitation is reached before 1.5min. For the material and geometry considered in this work the detection screen was placed in a vertical position, and σ_x = 3.5mm and σ_y = 4.1mm were measured. The screen infrared emissivity is 0.9.

The infrared camera used to explore the detector screen is a computer controlled 240 × 320 pixel PtSi FPA system refrigerated

with a Stirling microcooler. Its sensitivity, without frame averaging, is better than 0.1K.

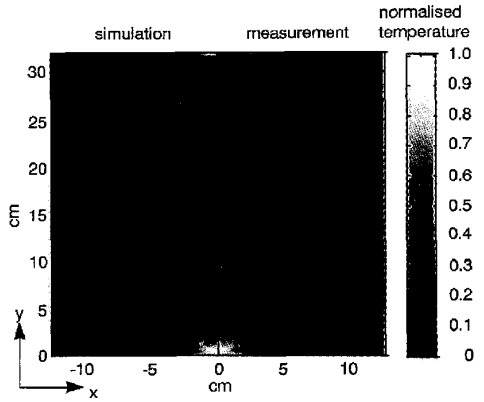

Fig. 3 *Prediction and measurement of 19cm high equilateral triangular wire antenna*

Left: prediction
Right: measurement
This Figure is shown in colour in Electronics Letters online

Experiments: The validity of the measurement method was assessed by comparing the measured results with numerical simulations. To increase the temperature of the lossy material by ~ 10–20K, a power of 5W at 2.45GHz was needed. The detection screen was 25cm wide and 32cm high. The thermal image generated by a monopole due to the tangential electric fields on the detection screen is presented in Fig. 2 in comparison with its predicted temperature increase over ambient temperature. The monopole is 1.5λ high and its diameter is 2.9mm and the detection screen is at 8mm from the monopole axis. Fig. 3 shows the simulated and thermal images on the detection screen of a 19cm high equilateral triangular antenna. The diameters of the wire used to construct the antenna and the measurement plane are 2 and 8mm, respectively.

Simulations for these structures were carried out in three phases: obtaining the current distribution on the antenna using the method of moments, evaluating the power densities absorbed by the detection screen, and performing a convolution with the hotspot response eqn. 2 of the material. Fig. 2 and Fig. 3 take advantage of the symmetry of simulations and real thermal images to simplify the representation of results. Therefore, the left half of the images, shows the predicted heating due to electric fields, while the right half shows real images. Images and colour bars are normalised to maximum temperatures on the detection screen.

Great similarity is observed between the predictions and real images acquired using the IR camera. Small magnetic losses of the resistive paper and discontinuities in the antennas are the main causes of differences between predictions and measurements.

Conclusions: Electromagnetic sensing with infrared thermograms is a quick, simple and economic technique useful for measuring induced fields in a noninvasive manner. With a suitable detection screen selection this technique is capable of electric or magnetic field inspection in very close proximity to radiating sources, where the traditionally used probes are more invasive. With the consideration of the material impulse response (eqn. 2) better correlation between predictions and measurements is found.

Acknowledgment: This work has been partially supported by the Spanish government through the grant TIC 96-0724-C06-04.

21 April 1999
Electronics Letters Online No: 19990655
DOI: 10.1049/el:19990655

J.M. González (*Signal Theory and Communications Area, Centro Politécnico Superior, Universidad de Zaragoza (UZ), C/María de Luna n. 3, 50015 Zaragoza, Spain*)

E-mail: arbesu@posta.unizar.es

A. Aguasca and J. Romeu (*Electromagnetics and Photonics Engineering Group, Department of Signal Theory and Communications, Universitat Politècnica de Catalunya (UPC), c/Gran Capità s/n, Mòdul D3 Campus Nord UPC, 08034 Barcelona, Spain*)

References

1 NORGARD, J.D.: 'Infrared/microwave correlation measurements', *Opt. Eng.*, 1994, **33**, pp. 85–96
2 NECATI ÖZISIK, M.: 'Heat conduction' (John Wiley & Sons, 1980)

Authentication and correction of digital watermarking images

Jaejin Lee and Chee Sun Won

A novel function for image watermarking is introduced. The proposed function gives a restoration/correction capability to image watermarking as well as the detection and localisation of alterations. The basic idea of the proposed watermarking technique is to adopt conventional error control coding techniques for generating a watermark.

Introduction: Since digital images are quite vulnerable to various attacks in computer network environments, watermarking techniques have been introduced to protect them. To date, three different functions for digital watermarks have been investigated [1]. In the first function, the ownership of the image is the main concern. Therefore, a robust invisible watermark which is difficult (or impossible) to remove is necessary for this function [2]. The second function of digital watermarking is to track the distribution of the images. This is closely related to the ownership function in the sense that the embedded watermarks are supposed to be robust to the attacks. However, the main purpose of the second function is to identify illegal distributors of images rather than to protect ownership. For the third function of watermarking, the watermark should be sensitive to identify changes in image and authenticate image content [1, 3]. In previous watermarking techniques for this image verification function, only a binary answer can be provided as to whether an image has been altered or not, or, at most, the locations of the modifications are identified. In this Letter, we expand the capability of the watermarking to correct the alterations as well. More specifically, we adopt an error control coding (ECC) technique to generate the watermark, which in turn makes it possible to correct and detect the changes from the extracted watermarks.

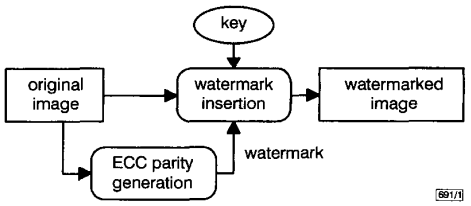

Fig. 1 *Embedding of invisible image watermarking*

Embedding the image watermark: In this Letter, we propose a novel method for correcting and identifying changes in the image data via the use of ECC techniques. The block diagram of the proposed watermarking process is given in Fig. 1. For the original image data, we first generate ECC codewords. For the ECC encoding, we can use the RS (Reed-Solomon) coding technique [4]. The generated ECC codewords' parities are then used as a watermark to be inserted into the image. At the receiver, as shown in Fig. 2, the watermark (i.e. ECC codewords) is extracted from the received watermarked image (changed or unchanged). The extracted ECC parities are then used to verify whether the image data have changed or not. If there are some changes in the watermarked image and they are within the error correction capability, the changes will be corrected by the ECC decoding to restore the original image data. However, if the number of changes exceeds the error correction capability, then the changes cannot be corrected but can still be detected and located.

Adopting RS encoding, the proposed watermarking can be more specifically described as follows. For a $K_1 \times K_2$ image, we first generate the RS codewords for each row. That is, for each